Journal of Alloys and Compounds, *187* (1992) 331–349
JALCOM 324

Chemical vapor deposition of silver films for superconducting wire applications

M. J. Shapiro*, W. J. Lackey and J. A. Hanigofsky
Georgia Tech Research Institute, Georgia Institute of Technology, Atlanta, GA (USA)

D. N. Hill and W. B. Carter
School of Materials Engineering, Georgia Institute of Technology, Atlanta, GA (USA)

E. K. Barefield
School of Chemistry and Biochemistry, Georgia Institute of Technology, Atlanta, GA (USA)

(Received November 18, 1991; in final form March 26, 1992)

Abstract

Chemical vapor deposition (CVD) was used to deposit silver films for superconducting wire applications. AgI, silver trifluoroacetate (Ag(TFA)), and perfluoro-1-methylpropenylsilver (Ag(PF)) produced the most promising silver films. CVD processing was optimized on these three precursors using thermodynamic calculations performed using a modified version of the SOLGASMIX-PV computer program. Ag(PF) produced the highest quality silver films at low temperatures and pressures. A fiber tow which contained a silver barrier layer and a $YBa_2Cu_3O_x$ overlayer was found to be a superconductor at 72 K.

1. Introduction

In order for the $YBa_2Cu_3O_x$ (YBCO) superconductor to be used to its full potential, it is necessary to produce high quality material, in the desired shapes, using practical fabrication methods. The weak-link problem [1, 2] of bulk YBCO is eliminated in thin films which have exhibited high critical current densities [3–7]. Barrier coatings between the superconductor and the substrate have allowed deposition of films with excellent properties for an increased number of substrates [8, 9].

Chemical vapor deposition (CVD) has been used to produce superconducting wire by depositing a thin film of YBCO on flexible ceramic fibers. One of the principal problems which must be overcome is the potential interaction between the YBCO and the ceramic filaments. A deposited silver film can act both as a passivation layer between the materials and as an outer coating which can be connected to electrical contacts. The goal of this investigation was to determine whether it is possible to produce a chemically vapor-deposited silver coating, which could be used both as a

*Present address: IBM, Hopewell Junction, NY, USA.

0925-8388/92/$5.00

barrier layer and as an overlayer for YBCO-coated filaments. Several possible silver-containing reagents were examined.

In order to infiltrate and coat completely a fiber bundle with silver, CVD must be used. Deposition of silver by conventional CVD has not been studied extensively. A silver film was produced by CVD on silicon using AgF as a reagent [10]. The film was deposited on silicon using the following overall reaction:

$$Si + 4AgF \longrightarrow 4Ag + SiF_4 \quad (1)$$

This vapor–solid reaction etched the sample as the deposition took place; the process has been demonstrated only on silicon substrates.

A brief description of the deposition of silver from silver trifluoroacetate (Ag(TFA)) $AgOOCCF_3$, using laser-assisted CVD was reported recently [11]. The Ag(TFA) was vaporized and deposited silver on various substrate surfaces.

Two other investigators have reported the possibility of using CVD for the deposition of group IB metals (which includes silver) employing metal complexes with cyclopentadienyl triethylphosphine [12, 13]. Both are patents, and all the experiments cited as examples utilized copper reagents and not silver.

The best silver films have been produced by plasma-enhanced CVD using silver perfluoro-1-methylpropenyl (Ag(PF)) AgC_4F_7 [14]. Silver films 20–500 nm in thickness were successfully deposited at rates of 6 nm min^{-1} on various substrates. Films made without an H_2 atmosphere contained polymeric substances as did films that were deposited at rates above 6.5 nm min^{-1}. The best films produced had resistivities of less than 2 $\mu\Omega$ cm and were close to 100% Ag.

The SOLGASMIX-PV program is commonly used to predict the compounds which are deposited in CVD experiments [15–17]. The model is more accurate for CVD systems in which the kinetics of the reaction and the diffusion of gases through the stagnation boundary layer are rapid [18–20]. The thermodynamic analysis indicates an upper boundary for the CVD process, which is ultimately controlled either by the kinetics or by the diffusion processes.

2. Procedure

2.1. Thermodynamic model

The computer program SOLGASMIX-PV [21, 22], a thermodynamic model, was used as a processing guide to aid in the selection of conditions that are most conducive to silver deposition. The effects of temperature, pressure, and composition on deposition were studied. SOLGASMIX-PV predicts the compounds which will be formed in an equilibrium process by minimizing the free energy of the total system.

The analysis was applied to CVD involving organometallic reagents as in a manner previously reported [23]. For the organometallic reagents for which no thermodynamic data were available, the assumption was made that

they decompose to simpler species at temperatures lower than the temperature of reaction.

The silver halides (AgF, AgCl, AgBr and AgI) were compared for ease of deposition, while AgI, Ag(TFA) and Ag(PF) were examined for the effect of temperature, pressure and H_2 concentration on processing. Data for the program included compounds to be considered, the enthalpy and entropy of the compounds at 1000 K, the temperature of reaction, the pressure and the molar amount of reference state materials. A temperature of 1000 K was valid to model thermodynamic values between 573 and 1473 K; variations in enthalpy and entropy were minimal over that range.

For each halide, a system of compounds which could possibly form and their associated thermodynamic data were assembled. Table 1 lists the compounds considered for each halide system. The enthalpy and entropy were found directly from the *JANAF Thermochemical Tables* [24] or they were calculated (values in tables indicated by a superscript b) using the following equations:

$$\Delta H^{\circ}_{1000\ \mathrm{K}} = \int_{298\ \mathrm{K}}^{1000\ \mathrm{K}} \Delta C_{\mathrm{p,\,f,\,T}}\,\mathrm{d}T - \Delta H^{\circ}_{298\ \mathrm{K}} \tag{2}$$

$$S^{\circ}_{1000\ \mathrm{K}} = \int_{298\ \mathrm{K}}^{1000\ \mathrm{K}} \frac{C_{\mathrm{p,\,T}}}{T}\,\mathrm{d}T - S^{\circ}_{298\ \mathrm{K}} \tag{3}$$

where ΔC_p is the heat capacity of the species, $\Delta H^{\circ}_{298\ \mathrm{K}}$ is the enthalpy of formation at 298 K of the species from the elements and $S^{\circ}_{298\ \mathrm{K}}$ is the entropy of the species at 298 K from the elements. Three references [25–27] were cross-checked to ensure accuracy. For some of the compounds, not all the thermodynamic data were available. In these cases an approximation was made (values in the tables indicated by a superscript c).

Thermodynamic data for organic species were needed for the Ag(TFA) system (Table 1) [28–30]. It was assumed that the organic compounds which formed during the reaction contained no more than two carbon atoms, since the Ag(TFA) compound contains only two carbon atoms per molecule. Most of the deposition runs were performed at 873 K, which would decompose larger molecules.

The Ag(PF) system contains the same elements as the Ag(TFA) system except that no O_2 is present. For the Ag(PF) system several compounds with larger carbon chains were included (Table 1). No thermodynamic data were available for $C_4F_7H(g)$, which was the most likely reduction product formed when Ag(PF) reacted with H_2. The reaction results in a substitution of a hydrogen atom for silver in the Ag(PF) compound. The enthalpy of formation and entropy for this compound were estimated from $C_4H_8(g)$ and fluorocarbon data. The SOLGASMIX-PV program was run with the estimated data and also with values $\pm 20\%$ of the original estimate. The results of the calculation did not differ, regardless of which values were used for $C_4H_8(g)$.

TABLE 1

Thermodynamic data used for SOLGASMIX-PV model

Species	$\Delta H^{\circ}_{1000\ K}$ (kJ mol^{-1})	$S^{\circ}_{1000\ K}$ (J mol^{-1} K^{-1})	
Ar(g)	0.000	183.789	For all systems
H_2(g)	0.000	171.790	
H(g)	223.346	143.660	
Ag(g)	271.586[a]	146.500[a]	
Ag(s)	0.000	73.470[a]	
HF(g)	−272.205	194.174	For F-containing
AgF(g)	118.868[a, b]	275.242[a, b]	reagents
F_2(g)	0.000	137.811	
F(g)	81.056	174.368	
AgF(s)	−166.387[a]	110.077[a]	
HCl(g)	−94.766	228.770	For AgCl
AgCl(g)	122.240[a]	288.020[a]	
Cl_2(g)	0.000	273.610	
Cl(g)	125.000	196.460	
AgCl(s)	−91.000[a]	157.620[a]	
HBr(g)	−54.018	235.032	For AgBr
AgBr(g)	125.588[a, b]	300.000[a]	
Br_2(g)	0.000	290.293	
Br(g)	98.028	200.301	
AgBr(s)	−62.857[a]	170.366[a]	
HI(g)	−5.961	227.233	For AgI
AgI(g)	125.819[a, b]	294.500[a, b]	
I_2(g)	0.000	289.000	
I(g)	76.000	197.000	
AgI(s)	−23.570[a]	181.290[a]	
C_2H_4(g)	44.310	258.870	For organic
CF_2O(g)	−641.000	297.740	reagents
CO(g)	−110.060	218.360	
CO_2(g)	−393.420	242.940	
CH_4(g)	−83.180	215.940	
CH_4O(g)	−210.420	277.260	
CF_4(g)	−933.350	313.540	
CHF_3(g)	−700.780	303.840	
CH_2O(g)	−120.630	247.120	
CH_2F_2(g)	−488.800	283.740	
CH_3F(g)	−241.520[c]	255.100	
C_2F_4(g)	−657.310	356.290	
C_2HF_3(g)	−789.810	350.620	
C_2H_2(g)	225.380	236.250	
H_2O(g)	−244.530	212.760	
H_2O_2(g)	−138.860	267.230	
C(s)	0.000	14.520	
Ag_2O(s)	−16.410	158.570	
Ag_2CO_3(s)	−481.080	230.120	
C_4H_8(g)	−26.620	376.320	Extra species
C_4F_7H(g)	−252.010[b]	592.140[a]	for Ag(PF)

[a]Value could only be found in one source [28].
[b]Calculated.
[c]Estimated.

Deposition diagrams and plots of partial pressure of gases formed were produced from the program. Deposition diagrams show the predicted deposited phases. To generate these diagrams, the temperature, the pressure and the $[H_2/([Ag]+[H_2])$ input gas ratio were varied.

2.2. Experimental details

Deposition was performed on various fibers and on flat polycrystalline Al_2O_3 substrates. Experiments where silver was deposited were performed in a vertical CVD furnace described elsewhere [31]. A powder-feed method to introduce the reagents into the furnace [32] was employed instead of conventional vaporization. This allowed lower vapor pressure materials to be used. Argon, flowing at 1 l min^{-1}, carried the reagent powders into the furnace.

Optimization experiments were performed using AgI, Ag(TFA) and Ag(PF). The experimental set-up was the same as the preceding investigation and each reagent was fed into the system for 20 min. Table 2 shows the H_2 flow rates, temperatures and pressures used.

The silver halides were purchased commercially in powder form and were at least 95% pure. The compounds included AgF, AgCl, AgBr and AgI; each was tested at deposition temperatures of 573 and 1173 K. Argon, flowing at 5 l min^{-1}, was used to transport 5 g of powder pneumatically into the furnace while H_2 at 1–10 l min^{-1} reduced the halides. The total pressure of the system was kept as low as possible, about 0.03 atm (2.67 kPa), to assist the vaporization of the reagent.

Two organometallic reagents containing silver, Ag(TFA) and Ag(PF), were also tested. The Ag(TFA) was purchased commercially while the Ag(PF) was synthesized at Georgia Tech using a method described elsewhere [33]. The conditions used were the same as the halide experiments except that the furnace temperature was 573 K. Both of these compounds were air sensitive and were handled in an argon-purged glove-bag.

All deposition experiments involving YBCO were performed in a horizontal furnace described elsewhere [31]. The procedure was designed to reduce diffusion of the silver into the substrate. Polycrystalline Al_2O_3 substrates coated with silver were held in a movable sample holder that was kept in

TABLE 2

Experimental conditions used for the optimization study

Reagent	H_2 flow rate (l min^{-1})	Temperature (K)	Pressure (kPa)
AgI	0, 2, 4, 6, 8, 10	1073, 1123, 1173	271, 36, 69
Ag(TFA)	0, 0.05, 0.075 0.1, 0.5, 1	573, 673, 773, 873, 973, 1073, 1173	2.7, 16, 29, 52, 65, 78
Ag(PF)	0, 0.045, 0.09, 0.135	573, 773, 973	4, 44, 71

the coolest part (below 773 K) of the three-zone furnace. When the furnace was heated to 1148 K, the samples were moved into the hot zone for deposition of the YBCO. Pressure was held at 0.03 atm (2.7 kPa) with flowing argon at 5 l min^{-1} and O_2 at 1 l min^{-1}. After about 5 min, deposition was halted, and the samples were again moved into the coolest part of the furnace. The samples were cooled in pure O_2 for 1 h. Some fiber samples that were coated with silver were run in a continuous fiber coater. The furnace and procedure have been described elsewhere [34].

Films of YBCO which had been tested and shown to be superconducting were coated with silver by CVD from Ag(PF) at a pressure of 0.04 atm (4.0 kPa) and a temperature of 573 K. Only part of the sample was coated with silver to allow for critical temperature testing. Partial coating was achieved by masking part of the YBCO surface with an MgO substrate. After deposition, some of the samples were annealed in O_2 at 823 K for 1 h.

2.3. Characterization

A Cwikscan model 100 scanning electron microscope was used to view both the surface and the cross-sections of the samples. Cross-sectioned samples were used to measure film thickness. Samples were analyzed for composition by energy-dispersive spectroscopy (EDS) using a Kevex model 1000 analyzer. X-ray diffraction (XRD) of the processed films was done with a Philips PW-1800 automated powder diffractometer using monochromatic Cu Kα radiation. Auger electron spectroscopy (AES) measured the relative amount of fluorine, oxygen and carbon that was retained in the silver films after deposition from organometallic precursors. Experiments were carried out with a Perkin–Elmer scanning auger multiprobe. The technique was qualitative, where scans were compared with a silver standard. Samples were first sputtered in the instrument in order to clean the surface of adsorbed species. Sputtering was done for 5 min using argon ions. The film thickness and roughness were measured using a Tracor Northern profilometer. Specimens were prepared by removing part of the coating with a razor blade. For thickness measurements, the stylus was placed on the film and traced across the sample from a coated to an uncoated area. Thickness measurements from the profilometer agreed with the scanning electron microscopy (SEM) measurements.

Resistance *vs.* temperature measurements were made utilizing a four-point probe method. Silver contacts were evaporated onto the specimens and thin copper wires were attached to these with conductive epoxy. Specimens were mounted on a cold finger capable of temperatures as low as 10 K. Specimen temperatures were monitored with a silicon diode. Mass spectrometry was performed with a VG analytical 70SE high resolution mass spectrometer which had a 11-250J data system. The collected exhaust gas from the CVD furnace was transferred from the glass collection vessel to the mass spectrometer with a gas syringe. The spectra obtained covered a range from 50 to 700 amu.

4. Results and discussion

4.1. Thermodynamic modeling

The different silver halide reagents were compared by the use of deposition diagrams (Fig. 1). The diagrams consist of a pure silver phase field and a silver-plus-silver-halide phase region when the temperature and pressure were varied. AgF has the largest two-phase region; deposition of pure silver was predicted at temperatures greater than 1100 K. For AgCl, the two-phase region consisting of silver and AgCl existed only below 940 K. The boundary line between the single- and two-phase regions decreases to a lower temperature at lower pressures. For AgBr and AgI, the two-phase regions were smaller for the same conditions when compared with the two previously discussed

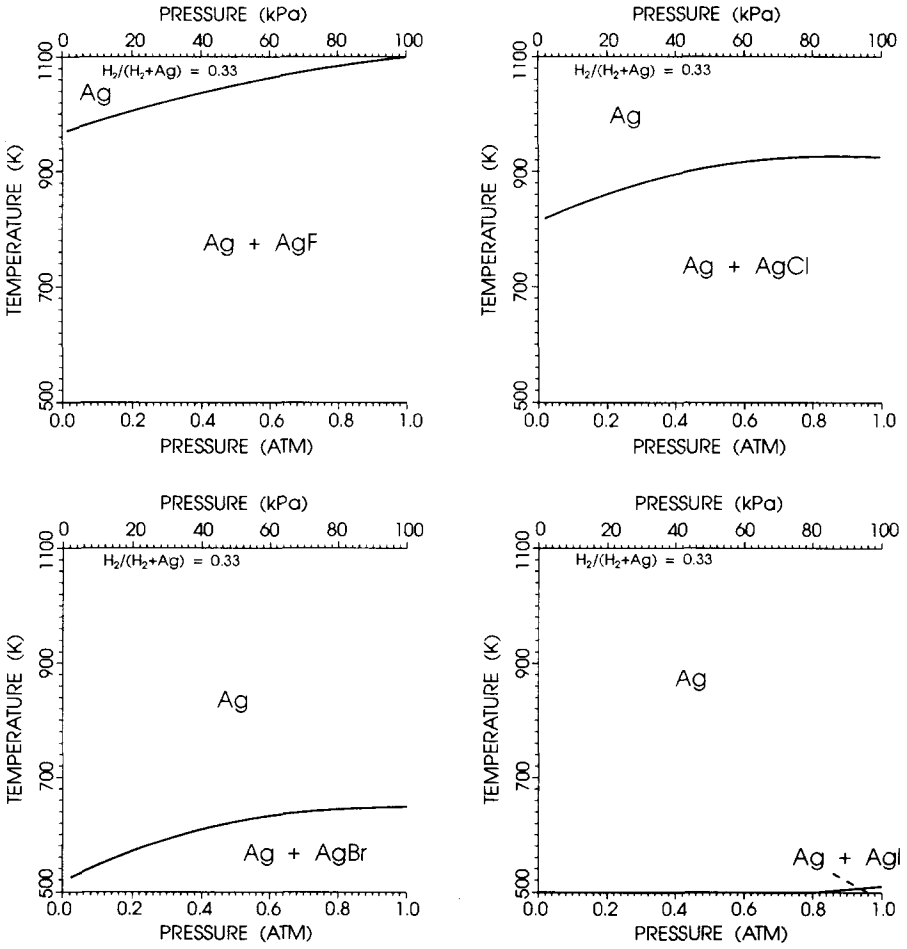

Fig. 1. Deposition diagrams comparing the silver halide reagents. The AgI has the largest single-phase region.

silver halides. The deposition diagrams indicate that the single-phase regions of silver increase in size as the atomic number of the halide element increases.

A deposition diagram (Fig. 2) generated from SOLGASMIX-PV shows the effect of $[H_2]/([H_2]+[Ag])$ and temperature. The diagram is dominated by a region of pure silver. The two-phase region of silver and AgI exists below 560 K for $[H_2]/([H_2]+[Ag])$ lower than 0.38. The diagram illustrates the importance of using excess H_2 while depositing silver from a silver halide.

The thermodynamic model predicts that silver and carbon are the only two condensed-phase products possible during CVD when Ag(TFA) is used as a reagent. A deposition diagram (Fig. 3) varies temperature and H_2 concentration. Both silver and silver-plus-carbon regions are present. At $[H_2]/([H_2]+[Ag])$ ratios below 0.14 and a temperature of less than 725 K a small two-phase region is present. Another two-phase area exists at higher hydrogen concentrations. Silver is thermodynamically stable at temperatures above 1120 K. The behavior observed in this deposition diagram can be explained with the partial pressure plot (Fig. 4) which is a section taken at 500 K on Fig. 3. The partial pressure of C_2HF_3 increases to a maximum at $[H_2]/([H_2]+[Ag])=0.5$. It is then depleted until none exists at a ratio of approximately 0.62. The presence of C_2HF_3 in Fig. 4 corresponds to the silver phase field at 500 K on Fig. 3. Much of the carbon from the Ag(TFA) is tied up in C_2HF_3 gas and hence is not available to form a solid. The diagram also shows that, as the H_2 concentration increases, the gas reacts with the fluorine to produce HF. The H_2 also combines with O_2. The compounds which contain carbon (CF_4, CF_2O and C_2HF_3) do not form at $[H_2]/([H_2]+[Ag])$ ratios above 0.62. The H_2 does form CH_4 with carbon but not enough to inhibit solid carbon from depositing.

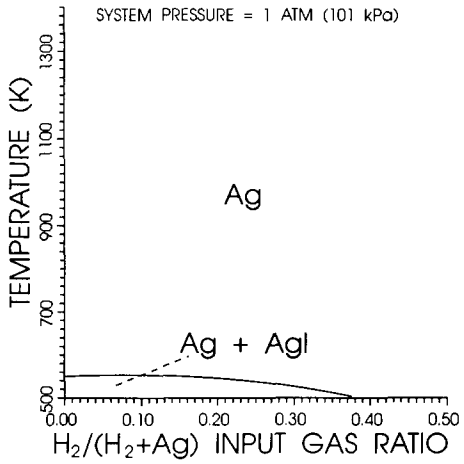

Fig. 2. The model predicts that increasing the H_2 concentration increases the likelihood of forming pure silver.

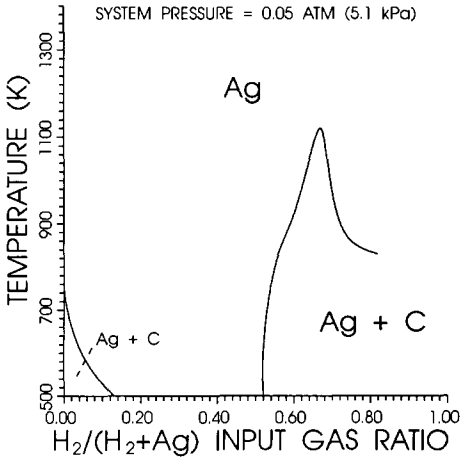

Fig. 3. Pure silver and silver-plus-carbon phase fields are predicted to deposit when Ag(TFA) is used as a reagent.

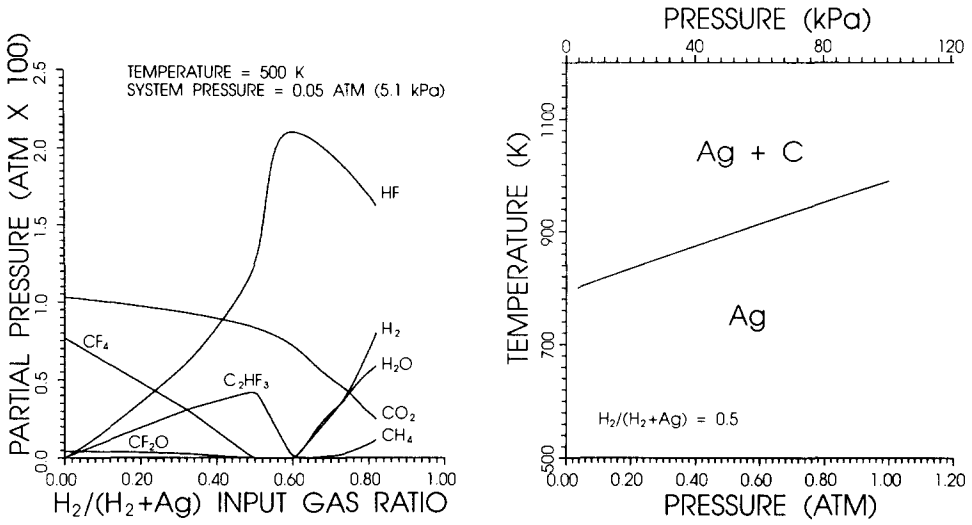

Fig. 4. The existence of C_2HF_3 in the gas phase corresponds with the pure silver region in Fig. 3.

Fig. 5. When Ag(PF) is used as a reagent, pure silver is predicted to form below 800 K, and silver-plus-carbon is predicted to form above 1000 K.

The thermodynamic model predicts that silver and carbon are the only phases which can be deposited from Ag(PF) for the conditions that were studied. Silver should exist only in the solid phase, giving 100% efficiency at all conditions investigated. Where carbon is predicted to deposit, silver is always present. A deposition diagram where temperature and pressure are varied (Fig. 5) shows the two types of phase region. A pure silver region is predicted to exist below 800 K. Above 1000 K the two phase silver-plus-carbon region exists. Increasing the total system pressure raises the temperature of the phase boundary line.

A partial pressure plot at 0.03 atm (2.7 kPa) (Fig. 6) can explain why carbon forms at high temperatures. At a temperature less than 700 K, C_2HF_3 remains constant in pressure at about 0.009 atm (900 Pa). As shown with Ag(TFA), C_2HF_3 is an important species for tying up free carbon. As the temperature increases above 700 K, HF and CF_4 become more stable which reduces the C_2HF_3 partial pressure. Excess carbon becomes available to form a solid. At higher total system pressures, C_2HF_3 becomes more stable with respect to temperature.

4.2. Reagent feasibility study

This study compared the thermodynamic analysis with actual deposition experiments. The SOLGASMIX-PV model correctly predicted the ease of deposition of the silver halides. The most complete deposition was achieved with AgI while AgF was the least successful reagent. A trend corresponding to the size of the region where silver exists in the predicted deposition diagrams (Fig. 1) was observed.

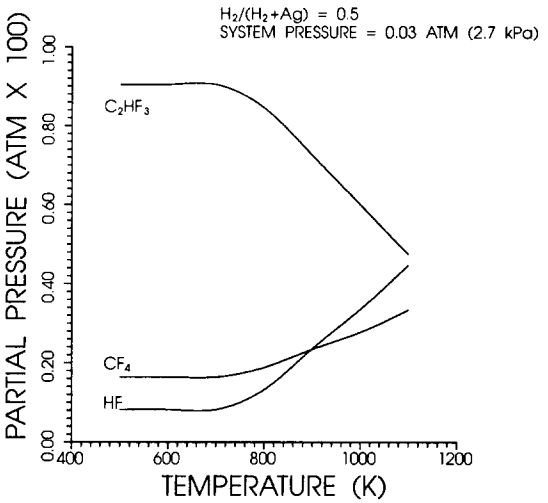

Fig. 6. High partial pressures of C_2HF_3 gas correspond with the pure silver phase field in Fig. 5.

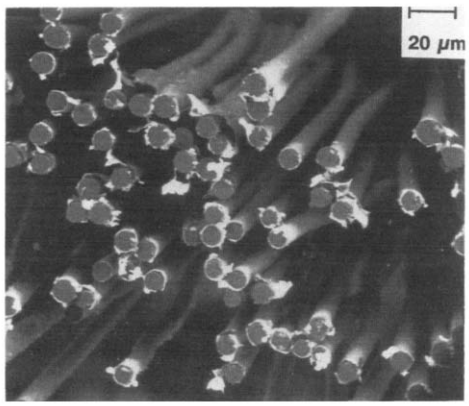

Fig. 7. Micrograph showing a fiber tow that is completely infiltrated. Each individual filament is coated with a silver film.

4.3. AgI study

The feasibility study and thermodynamic model both indicated that AgI was the halide most likely to form a silver film by CVD. No silver film could be formed at temperatures below 973 K or at pressures greater than 0.80 atm (80 kPa). The best film was deposited at a temperature of 1073 K and a pressure of 0.03 atm (2.7 kPa). The XRD analysis revealed that the silver phase was dominant with the only other peaks being due to the Al_2O_3 substrate. The film was smooth and continuous as determined by SEM investigations. All other coating conditions produced spotty films or no silver. Also, infiltration of silver into a fiber tow was never achieved using AgI, although it was with other silver halides (Fig. 7).

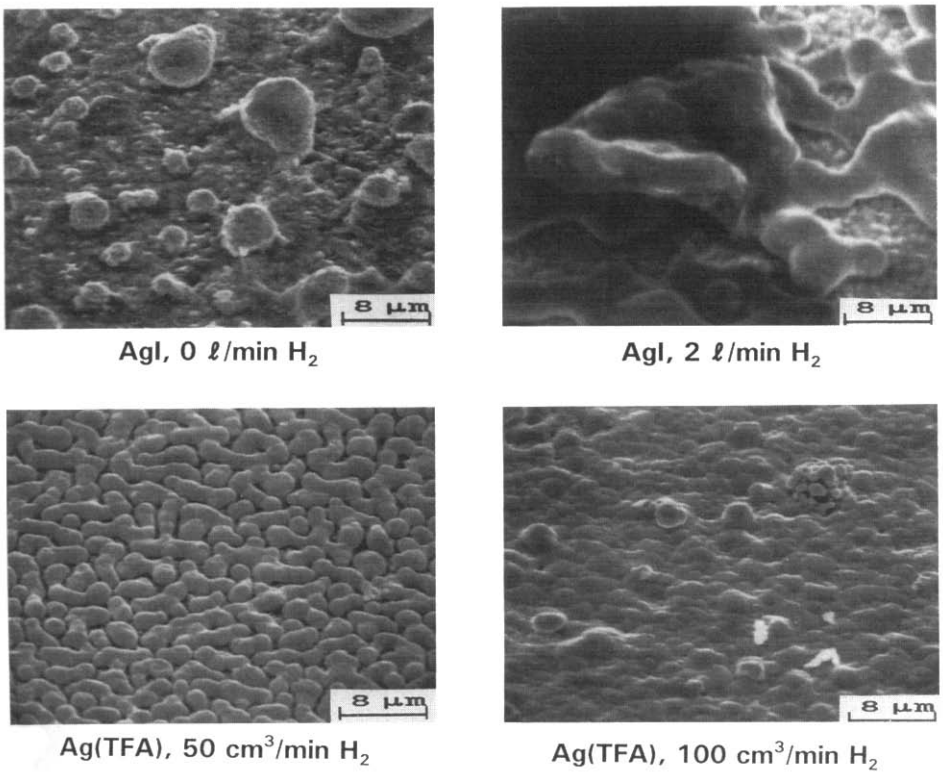

Fig. 8. SEM images showing the effect of increasing H_2 flow on deposition from AgI and Ag(TFA). More H_2 increases the continuity of the resulting silver films.

The amount of H_2 used in the deposition of silver from AgI was found to be a significant factor effecting thickness. Figure 8 compares deposits produced at 0 and 2 l min^{-1}. Only small silver nodules were deposited when no H_2 was added to the system; most of the substrate was uncoated. At a H_2 flow of 2 l min^{-1}, a more continuous film was produced. At higher H_2 flows, the films completely coated the substrate, as reported in previous CVD efforts with halide compounds [16].

The thermodynamic model predicted that at the temperature used no H_2 gas is needed to produce a pure silver film. The experiment confirms this since no other phases were detected in the XRD patterns and silver films were produced at every condition. However, a small amount of iodine was observed by EDS as being present in the film when no H_2 was used. The iodine was most probably present in solution in the silver film. The SOLGASMIX-PV model could not be programmed for prediction of solid solutions since these data do not exist.

4.4. Silver trifluoroacetate

The best silver films deposited using Ag(TFA) were produced at 873 K with a H_2 flow rate of 1 l min^{-1}. Lowering the temperature from 873 K

increased the roughness of the films and caused large clumps of grains to form. Temperatures above 873 K produced a slightly more porous microstructure. Since lower temperatures are desired for the deposition of silver with YBCO, the temperature of 873 K was selected as being the most desirable. Profilometry showed that the silver films were approximately 2 μm thick which corresponds to a coating rate of 6 μm h^{-1}. The system pressure did not affect the deposition for this reagent.

Varying the amount of H_2 had a considerable effect on the deposition process (Fig. 9). The thickness of the films increased as the H_2 partial pressure increased. Two-point resistance measurements showed that, at H_2 flow rates of 0.05 l min^{-1} and below, the silver films were insulating. SEM showed that these films were discontinuous. Micrographs of two silver films prepared with H_2 flows of 0.05 and 0.10 l min^{-1} are shown in Fig. 8. The sample with the higher H_2 flow rate (0.10 l min^{-1}) is continuous with slight porosity. The other specimen (0.05 l min^{-1}) shows a discontinuous microstructure and a high resistance. XRD and AES did not detect any impurity phases or elements in the films. On the basis of the XRD, SEM, and profilometry results, it is apparent that higher H_2 flows increase the efficiency of the deposition by enhancing the Ag(TFA) decomposition.

The model successfully predicts the behavior of Ag(TFA) at temperatures above 1223 K. For all experiments conducted above this temperature, silver was the only phase to form. At lower temperatures, the model breaks down with respect to pressure and H_2 concentration. Experiments show that, in all cases, silver was produced regardless of the deposition conditions. The model predicted that carbon was expected to be present in the films, but it was never observed. AgF, Ag_2O and Ag_2CO_3 solids were never predicted to form and these phases were also never detected.

Additional experiments were performed with deposition conditions selected to fall in as yet unexplored regions of the predicted deposition diagram. Still only silver was deposited. Carbon was most probably not present in the films because the Ag(TFA) molecule never dissociated fully. Adding H_2

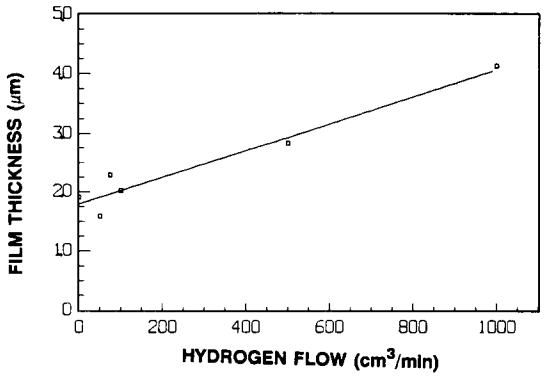

Fig. 9. The effect of H_2 flow rate on the thickness of silver films produced from Ag(TFA). The curve was fitted to the data.

and heating the Ag(TFA) to temperatures of 873 K or less probably caused only a partial break-up of the molecule. This allowed silver but not carbon to dissociate and become a solid. At higher temperatures, the molecule dissociates more completely but, at these temperatures (above 1223 K), no carbon was expected in the film. Dissociation kinetics are slower at lower temperatures; so this would be an expected behavior. Even if solid carbon did form, it may not have been incorporated in the film. Solid phases can form and have a low sticking coefficient. This allows the solid to be entrained in the gas phase and flow out of the CVD system. No evidence of carbon powder was found in the downstream side of the CVD reactor; so this mechanism is unlikely.

4.5. Perfluoro-1-methylpropenylsilver tests

Ag(PF) produced the highest quality silver films in the initial reagent tests. The best coatings on flat Al_2O_3 substrates were achieved at 973 K and 0.04 atm (4.0 kPa). Fibers were better infiltrated at 573 K and 0.04 atm (4.0 kPa).

The coating rate and infiltration of the silver films produced from Ag(PF) were dependent on temperature and pressure. Every experiment run in this study produced some silver deposit on the Al_2O_3 substrates. Of these, two thirds of the films were continuous or semicontinuous as determined by SEM. All films were polycrystalline with no preferred orientation.

Coatings produced at various pressures and temperatures are compared in Fig. 10. The thickness of the silver film was about 2.2 μm for the sample processed at 973 K and 0.04 atm (4.0 kPa). This corresponds to a coating rate of 6.6 $\mu m\ h^{-1}$. An increasing amount of pores existed for films produced at lower temperatures at the same pressure. At 573 K the coating rate was 5.4 $\mu m\ h^{-1}$. Only spots of silver were deposited on the Al_2O_3 substrate when the conditions used were 773 K and 0.83 atm (84 kPa). Similar coatings were deposited at 973 K at pressures of 0.43 and 0.83 atm (44 and 84 kPa). All the films produced at 573 K were similar regardless of pressure.

The variation in the amount of coating observed in this experiment with changes in processing temperature and pressure agrees with CVD theory. As the pressure is lowered, the stagnation boundary layer at the substrate decreases in thickness. The gas must diffuse across this layer to produce a deposit on the substrate. At high pressures, the diffusion distance is large and less material is deposited. Experimentally, the lowest pressure, 0.04 atm (4.0 kPa), gave the greatest amount of coating as would be anticipated from boundary layer theory. Increasing temperature also increases the diffusion of the gas through the stagnation region. The results exhibit this behavior at a pressure of 0.04 atm (4.0 kPa); however, at higher pressures the amount of coating does not significantly differ for differences in temperature. Another possible explanation of the temperature and pressure effects on deposition is the occurrence of homogeneous nucleation. At high temperatures and pressures it is possible for reagents to react in the gas phase and to form

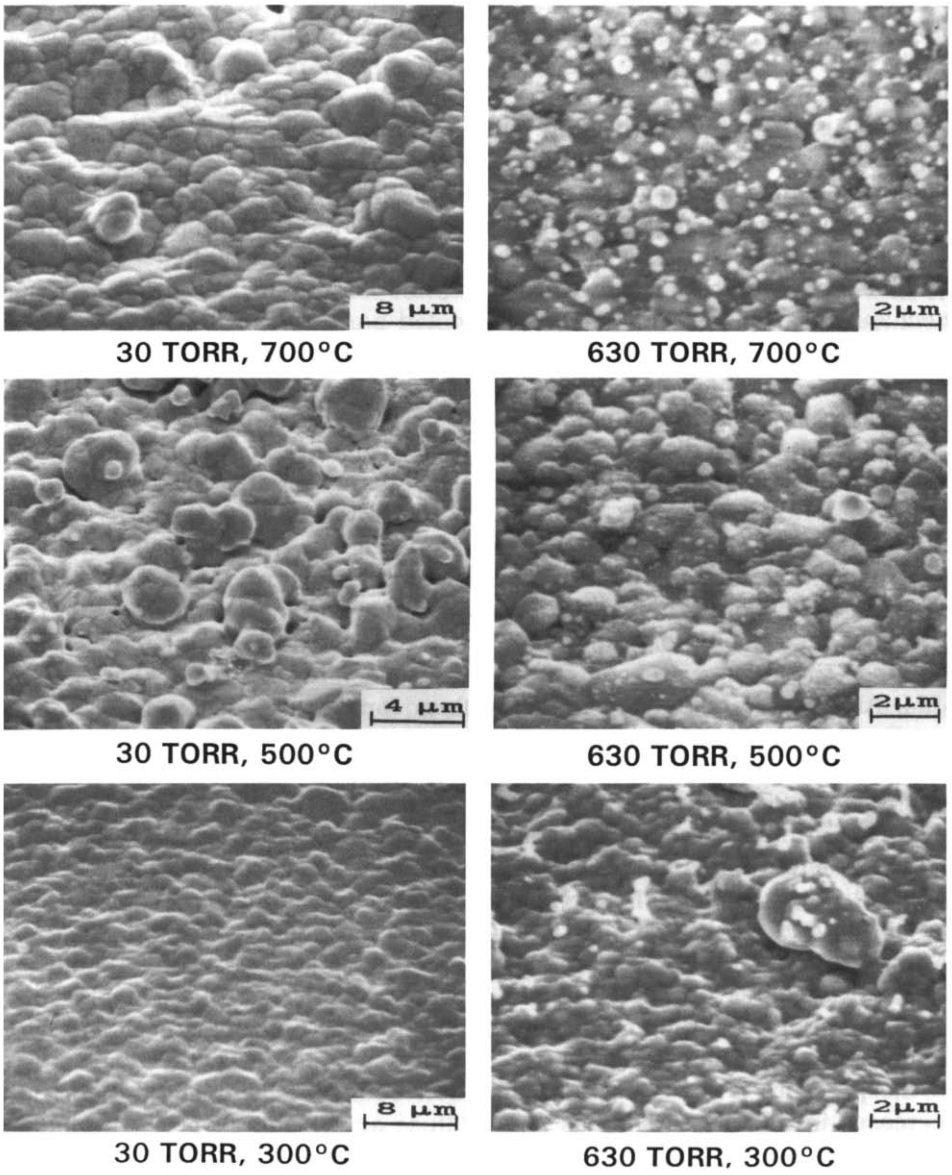

Fig. 10. Micrographs illustrating the effect of temperature and pressure on the deposition of silver using Ag(PF). Lower pressures produced higher quality silver films.

a powder. The powder may only sparsely deposit on the substrate as seen in Fig. 10.

The deposition of silver from Ag(PF) was not affected by varying the amount of H_2. SEM showed that all the films produced had similar microstructures. Although the grain size varied from sample to sample, no correlation could be found between grain size and H_2 flow. The films were uniform and

had little to no porosity. Profilometer measurements indicated coating thicknesses of 1–2 μm for all samples. No chemical impurities were found in the sputtered specimens by AES. The experiments run with no H_2 and H_2 at 0.010 l min^{-1} were inconclusive. In both cases, AgO was found in the film by XRD.

The model predicted that silver would be produced from Ag(PF) under all the deposition conditions studied. Experiments confirmed this prediction. Also, AgF was never detected in the films, again in agreement with the SOLGASMIX-PV prediction. However, the model also predicted that solid carbon would form in many instances. The AES spectra of the sputtered samples from the above studies matched the spectrum of the sputtered pure silver specimen. Extra experiments were done to map more fully the predicted deposition diagrams, and still no carbon was present. Even though the model had predicted the H_2 concentration to be important, experiments revealed that carbon was undetectable regardless of H_2 flow.

Mass spectrometry indicated that the model was incorrect with respect to the gases that were formed during deposition. The mass spectra taken from runs at 0.04 and 0.43 atm (44 kPa) were similar, with the important feature being the species at 182 amu which corresponds to C_4F_7H. This compound is formed by substitution of hydrogen for silver in Ag(PF). SOLGASMIX-PV did not predict the existence of the olefin under any condition. It was always broken down to simpler species which had a combined free energy that was lower than that of C_4F_7H. Apparently, kinetics did not allow thermodynamic equilibrium to be achieved. The kinetics were expected to be slow since the deposition was performed at 573 K. C_4F_7H did form and tied up elemental carbon in the gas phase.

4.6. $YBa_2Cu_3O_x$

Films of YBCO were successfully deposited on silver-coated polycrystalline Al_2O_3 substrates. XRD indicated that the YBCO films were randomly oriented (Fig. 11). The highest intensity silver peak also was present in the pattern, showing that it all did not diffuse into the substrate. Previous work had shown that barium aluminate would form between uncoated Al_2O_3 and YBCO. No barium aluminate was observed in the XRD pattern when silver was used as a buffer layer. The two-point resistance of these samples varied from 5 to 500 Ω. SEM revealed a fine-grained structure for the YBCO, which is undesirable. Two samples were tested for superconducting transitions but both exhibited semiconducting behavior. Another sample was annealed at 1023 K in an O_2 partial pressure of 0.005 atm (0.053 kPa) and at 773 K for an extra 1 h in O_2 at 1 atm (101 kPa). The sample had a two-point resistance which was less than 0.1 Ω. The four-point resistance of the sample was measured in the microhm range. The sample was unsuccessfully tested for a superconducting transition because the experimental set-up was not sensitive enough to measure the low resistivity of the sample. The silver most probably diffused into the grain boundaries of the YBCO and formed a continuous network, leading to the low resistance in the sample.

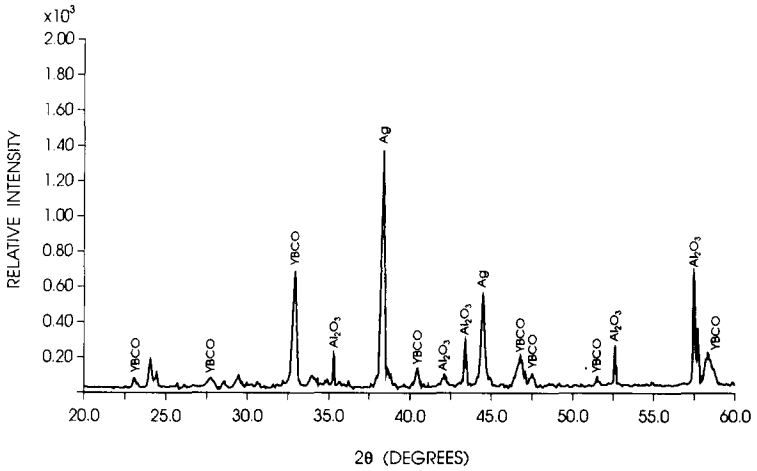

Fig. 11. XRD indicates that randomly oriented YBCO was deposited on top of the silver film.

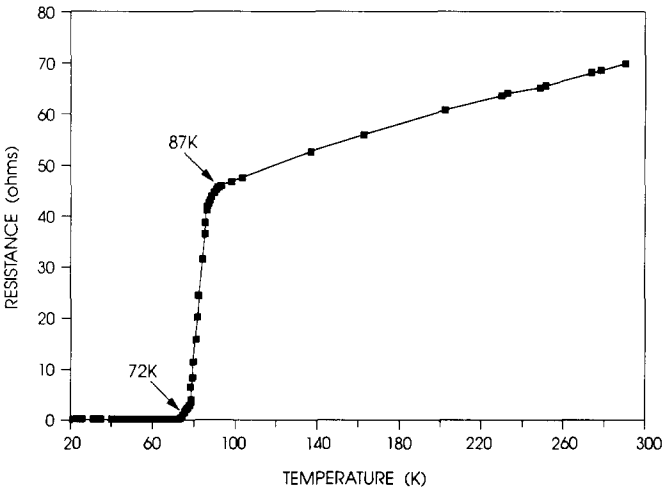

Fig. 12. A fiber tow with YBCO coated onto a silver film was superconducting at 72 K.

One silver-coated fiber sample that was subsequently coated with YBCO and annealed in O_2 for 16 h at 823 K did become superconducting at 72 K (Fig. 12). Many other samples receiving the same treatment were superconducting at slightly lower temperatures. It is clear that the silver was a critical factor in producing the superconducting samples since identically processed fibers without a silver film were not superconducting. It is known that the YBCO will react unfavorably with the Al_2O_3 fiber at the process temperature used. The silver appeared to serve as a barrier layer to prevent the interaction.

4.7. Silver deposition on $YBa_2Cu_3O_x$

Silver was easily deposited on top of YBCO films using Ag(PF) as a reagent. The deposition was done at 573 K at a pressure of 0.03 atm (2.6 kPa) to try to minimize oxygen loss from the superconductor. The original and YBCO post-silver-deposition film was oriented with the *c* axis perpendicular to the single-crystal MgO substrate. Silver peaks were also present in the XRD pattern. A concern was that the oxygen in the YBCO would diffuse out of the structure when subjected to the highly reducing environment used to deposit the silver. XRD was used to check this by calculating the lattice cell volume. The cell volume has been shown to increase as the amount of oxygen in the YBCO decreases [35]. Silver-coated samples had an average cell volume of about 0.176 nm^3, which corresponds to an oxygen content of under 6.1. The samples began with an oxygen content above 6.6; so they were reduced by the silver coating process. The deposited silver film was fine grained with overlapping porous layers. EDS indicated the film was pure silver. Samples that were annealed in O_2 after deposition were not superconducting when tested at temperatures down to 77 K. Some did display ohmic behavior and began to have a resistive transition just above 77 K.

5. Conclusions

Both Ag(TFA) and Ag(PF) were shown to be capable of producing silver barrier layers for YBCO on Al_2O_3-containing fibers. AgI would only be usable with flat substrates, since it was not possible to infiltrate fiber tows with silver. The fastest deposition rate, over 300 $\mu m\ h^{-1}$, was achieved with AgI. This rate is at least 50 times more rapid than that for the organometallic reagents. Ag(TFA) and Ag(PF) produced much smoother films on which subsequent deposition of YBCO would be easier. Since Ag(TFA) was the less expensive of the two compounds, it is the most likely candidate for producing silver barrier layers. The highest quality films were deposited at 873 K with a reagent powder feed rate of 0.15 g min^{-1} and with H_2 flowing at 1 l min^{-1} at a pressure of 0.03 atm (2.6 kPa). The best fiber infiltration from Ag(TFA) was shown to occur at the lowest pressures used of 0.04 atm (4.0 kPa).

Initial superconductivity tests of the silver barrier layer on flat Al_2O_3 and Al_2O_3-containing fibers show that superconducting samples can be produced. One multifilament fiber sample exhibited superconductivity at 72 K. The flat samples all had low resistances which made four-point resistance testing difficult. None of the flat specimens studied was shown to be superconducting at 77 K. The silver layer most probably prevented the reaction of the YBCO and the Al_2O_3 substrate.

Ag(PF) produced silver films at the lowest temperature of 573 K and infiltrated fiber tows more completely than the other reagents investigated. Low temperature deposition allows the silver films to be deposited onto YBCO films without poisoning the superconductor with CO and/or CO_2.

However, since deposition is done in severely reducing conditions, reoxygenation of the YBCO was needed. Since the presence of H_2 was found not to be significant, it may be possible to deposit the Ag(PF) in an O_2 environment. Ag_2O probably would form at 573 K, but thermodynamic calculations indicate that at higher temperatures Ag_2O would not be stable. YBCO is known to take up O_2 at 723–823 K.

The thermodynamic model was a valuable guide for selection of deposition conditions. Experimental evidence agreed with the model prediction that AgI was the most effective halide reagent. The other silver halides also were arranged in order of ease of deposition: AgBr, AgCl and AgF. The need for excess H_2 with halide deposition also was accurately predicted by SOLGASMIX-PV.

The thermodynamic model was not as helpful with the organometallics. It did correctly predict that the only silver-containing phase to deposit would be pure silver, and that it would form in every condition tested. This meant AgF, Ag_2O and Ag_2CO_3 were not a concern. SOLGASMIX-PV predicted that carbon would form in many instances, but no carbon was found experimentally. Since the model assumes that all reactions go to thermodynamic equilibrium which is more likely at higher temperatures, this discrepancy was not unexpected. In the case of Ag(PF), where low temperatures were used and equilibrium may have not been achieved, it was shown that the carbon-containing molecule was not dissociating completely which was expected from the thermodynamic calculations. Even so, the model presents a worst-case scenario for deposition. If silver is the only element which dissociates from the Ag(PF) molecule, deposition parameters can vary widely with little effect. If the molecule did break up more completely, the thermodynamic model would have been an accurate guide to selection of processing conditions.

References

1 P. Chaudhari, J. Mannhart, D. Dimos, C. C. Tsuei, J. Chi, M. M. Oprysko and M. Scheuermann, *Phys. Rev. Lett., 60* (1988) 1653.

2 D. Dimos, P. Chaudhari, J. Mannhart and F. K. LeGoues, *Phys. Rev. Lett., 61* (2) (1988) 219–22.

3 X. X. Xi, G. Linker, O. Meyer, E. Nold, B. Obst, F. Ratzel, R. Smithey, B. Strehlan, F. Weschenfelder and J. Geerk, *Z. Phys. B, 74* (1989) 13.

4 D. Kijkkamp, T. Venkatesan, X. D. Wu, S. A. Shaheen, N. Jisrawi, Y. H. Min-Lee, W. L. McLean and M. Croft, *Appl. Phys. Lett., 51* (1987) 619.

5 D. K. Lathrop, S. E. Russek and R. A. Buhrman, *Appl. Phys. Lett., 51* (1987) 1554.

6 T. Terashima, K. Iijima, K. Yamamoto, Y. Bando and H. Mazaki, *Jpn. J. Appl. Phys., 27* (1988) L91.

7 H. Yamane, H. Kurosawa and T. Hirai, *Proc. 7th Eur. Conf. on Chemical Vapour Deposition, Perpignan, France, June 1989*, Les Editions de Physique, 1989, pp. C5 131–140.

8 A. Mogro-Campero and L. G. Turner, *Appl. Phys. Lett., 53* (1988) 2566.

9 K. Fujino, *Jpn. J. Appl. Phys., 28* (1989) L236.

10 R. J. H. Voorhoeve and J. W. Merewether, *J. Electrochem. Soc., 119* (1972) 364.

11 Anon., *Res. Discl., 263* (1986) 146.

12 A. Erbil, Chemical vapor deposition of group IB metals, *US Patent 4, 880, 670*, November 14, 1989.

13 D. B. Beach, J. M. Jasinski and E. M. Kreidler, Method for chemical vapor deposition of copper, silver, and gold using a cyclopentadienyl metal complex, *Eur. Patent Appl. 0 297 348 A1*.
14 C. Oehr and H. Suhr, *Appl. Phys. A, 49* (1989) 691–696.
15 R. G. Behrens, L. R. Newkirk and T. C. Wallace, Thermodynamics of the tantalum–carbon–chlorine–hydrogen system applied to the CVD of carbide/carbon materials, *Proc. 82nd Annu. Meet. of the American Ceramic Society*, in *Rep. LA-UR-80-1252*, (1980) (Los Alamos Scientific Laboratory, Los Alamos, NM) (US Department of Energy Contract).
16 M. S. Wang and K. E. Spear, in McD. Robinson, G. W. Cullen, C. H. J. Van den Brekel and P. Rai-Choudhury (eds.), *Proc. 9th Int. Conf. on Chemical Vapor Deposition*, Electrochemical Society, Pennington, NJ, 1984, pp. 98–111.
17 D. J. Twait, W. J. Lackey, A. W. Smith, W. Y. Lee and J. A. Hanigofsky, *J. Am. Ceram. Soc., 73* (1990) 1510.
18 A. I. Kingon, L. J. Lutz and R. F. Davis, *J. Am. Ceram. Soc., 66* (1983) 551.
19 A. I. Kingon, L. J. Lutz, P. Liaw and R. F. Davis, *J. Am. Ceram. Soc., 66* (1983) 558.
20 G. S. Fischman and W. T. Petuskey, *J. Am. Ceram. Soc., 68* (1985) 185.
21 G. Eriksson, *Chem. Scr., 8* (3) (1975) 100.
22 T. Besmann, SOLGASMIX-PV, a computer program to calculate equilibrium relationships in complex chemical systems, *ORNL Tech. Memo. TM-5775*, 1977 (Oak Ridge National Laboratory, Oak Ridge, TN, 37830).
23 C. Vahlas and T. Besmann, *Proc. 11th Int. Conf. on Chemical Vapor Deposition*, Electrochemical Society, Pennington, NJ, 1990, pp. 188–194.
24 D. R. Lide, Jr. (ed.), *JANAF Thermochemical Tables*, 3rd edn., Vols. I and II, American Chemical Society and American Institute of Physics for National Bureau of Standards (US), 1985.
25 I. Barin, O. Knacke and O. Kubaschewski, *Thermochemical Properties of Inorganic Substances: Supplement*, Springer, Berlin, 1977.
26 M. Kh. Karapet'yants and M. L. Karapet'yants, *Thermodynamic Constants of Inorganic and Organic Compounds*, Humphrey Science Publishers, Ann Arbor, MI, 1970.
27 K. Schäfer and E. Lax (eds.), *Eigenschaften der Materie in Inhren Aggregatzuständen*, Springer, Berlin, 1961.
28 J. D. Cox and G. Pilcher, *Thermochemistry of Organic and Organometallic Compounds*, Academic Press, London, 1970.
29 D. R. Stull, E. F. Westrum, Jr. and G. C. Sinke, *The Chemical Thermodynamics of Organic Compounds*, Wiley, New York, 1969.
30 J. B. Pedley, R. D. Naylor and S. P. Kirby, *Thermochemical Data of Organic Compounds*, Chapman and Hall, London, 1986.
31 W. Y. Lee, W. J. Lackey, G. B. Freeman, P. K. Agrawal and D. J. Twait, Preparation of dispersed phase ceramic BN+AlN composite coatings by chemical vapor deposition, *J. Am. Ceram. Soc., 74* (9) (1991) 2136.
32 W. J. Lackey, W. B. Carter, J. A. Hanigofsky, D. N. Hill, E. K. Barefield, G. Neumeier, D. F. O'Brien, M. J. Shapiro, J. R. Thompson, A. J. Green and T. S. Moss III, *Appl. Phys. Lett., 56* (1990) 1175.
33 F. L. Whiting, G. Maman and J. P. Young, *J. Am. Chem. Soc., 91* (1969) 6532.
34 J. A. Hanigofsky, Thesis, Georgia Institute of Technology, Atlanta, GA, 1992.
35 N. Wong-Ng, R. S. Roth, L. J. Swartzendruber, L. H. Bennett, C. K. Chiang, F. Beech and C. R. Hubbard, *Adv. Ceram. Mater., 2* (1987) 565–576.